



Pt/C catalysts with narrow size distribution prepared by colloidal-precipitation method for methanol electrooxidation

Shikui Yao^{a,c}, Ligang Feng^{a,c}, Xiao Zhao^{a,c}, Changpeng Liu^b, Wei Xing^{a,*}

^a State Key Laboratory of Electroanalytical Chemistry, Changchun Institute of Applied Chemistry, 5625 Renmin Street, Changchun 130022, PR China

^b Laboratory of Advanced Power Sources, Changchun Institute of Applied Chemistry, 5625 Renmin Street, Changchun 130022, PR China

^c Graduate School of the Chinese Academy of Sciences, Beijing, PR China

H I G H L I G H T S

- Colloidal-precipitation method was explored to prepare Pt/C.
- The prepared Pt nanoparticles dispersed well and had a narrow size distribution.
- Particle size of the Pt can be well controlled.
- The Pt/C showed enhanced activity and stability for methanol electrooxidation.

A R T I C L E I N F O

Article history:

Received 30 March 2012

Received in revised form

29 May 2012

Accepted 31 May 2012

Available online 9 June 2012

Keywords:

Direct methanol fuel cells

Colloidal-precipitation method

Anode catalyst

Methanol electrooxidation

A B S T R A C T

A simple, environment-friendly and aqueous-route colloidal-precipitation method is successfully employed to prepare carbon supported platinum nanoparticles with a narrow size distribution. In this method, $(\text{NH}_4)_2\text{WO}_4$ is used to react with H_2PtCl_6 , which forms the $(\text{NH}_4)_2\text{PtCl}_6$ and H_2WO_4 simultaneously. The precipitation of $(\text{NH}_4)_2\text{PtCl}_6$ and the colloidal of H_2WO_4 can protect the formation of the Pt nanoparticles. Transmission electron microscopy demonstrates that the Pt nanoparticles with a narrow size distribution are well dispersed on the carbon support. More importantly, the size of the Pt nanoparticles can be simply controlled by tuning the concentration of $(\text{NH}_4)_2\text{WO}_4$ and the Pt nanoparticles prepared in the 0.5 mmol L^{-1} $(\text{NH}_4)_2\text{WO}_4$ exhibit the smallest size of ca. 3 nm. Further, cyclic voltammetric and chronoamperometric experiments show that the prepared Pt/C catalyst exhibited excellent catalytic activity and stability compared with the Pt/C prepared by impregnation method and the state-of-the-art commercial Pt/C. For example, the peak current and the stable current at 3600 s of the Pt/C catalyst prepared with the 0.5 mmol L^{-1} $(\text{NH}_4)_2\text{WO}_4$ is about 1.24 and 1.78 times of the commercial Pt/C. Therefore, the as-proposed colloidal-precipitation method exhibits a potential application in preparing highly dispersive and electroactive Pt/C catalysts for direct methanol fuel cells.

© 2012 Elsevier B.V. All rights reserved.

1. Introduction

Direct methanol fuel cells (DMFCs) are considered to be the promising candidates for portable devices and vehicle applications due to their high energy density, easy manipulation and high efficiency [1–3]. From a technical point of view, the low activity and poor stability of the anode catalysts toward methanol electrooxidation still hinder the commercialization of DMFCs [1–4]. Therefore, intensive researches have been carried out to prepare high activity catalysts for methanol electrooxidation.

The preparation of catalysts with high performance for methanol oxidation should consider both the catalyst composition and preparation method. The most efficient anode catalyst used for the electrooxidation of methanol is carbon supported Pt or Pt–Ru [5–8]. Preparation method also influences the structure and morphology of the catalysts obviously, such as the average size, the alloying extent of the metal and the electrochemical active surface area, which can significantly affect the final electrocatalytic properties for the catalysts [9]. Much work has been devoted to study the preparation method for the catalysts [10–25]. For example, the impregnation method and the colloidal method are generally adopted. The impregnation process is, by far, the most attractive synthetic route due to its simplicity. However, the application is also limited by the large average metal particle size, the broad size

* Corresponding author. Tel.: +86 431 85262223; fax: +86 431 85685653.
E-mail address: xingwei@ciac.jl.cn (W. Xing).

distribution and poor reproducibility. By contrast, the particles size and size distribution can be controlled easily by the colloidal method [26–28]. Bonnemant et al. [29] developed an organometallic colloid route by stabilizing the Pt/Ru metal particles with organic molecules, the prepared Pt/Ru catalysts showed comparable activity ($\sim 70 \text{ mA mg}^{-1}_{\text{PtRu}}$) at 500 mV (versus RHE) in $0.5 \text{ mol L}^{-1} \text{ CH}_3\text{OH} + 0.5 \text{ mol L}^{-1} \text{ H}_2\text{SO}_4$ at 60°C with that of state-of-the-art Pt/Ru ($\sim 80 \text{ mA mg}^{-1}_{\text{PtRu}}$) at the same conditions), while further improvement is also expected due to the complexity of the preparation steps and the relatively high cost of those colloid routes.

In this paper, uniform Pt nanoparticles were prepared by a novel colloidal-precipitation method. Briefly, $(\text{NH}_4)_2\text{WO}_4$ was used to react with H_2PtCl_6 , the products of $(\text{NH}_4)_2\text{PtCl}_6$ and colloid of H_2WO_4 [18] worked together to control the formation of Pt nanoparticles. The Pt/C catalysts were characterized by physical and electrochemical experiments. The EDX results indicated that inorganic W species can be removed simply by washing with excessive water. The as-prepared Pt/C catalysts had a small average particle size with a narrow size distribution, and moreover, the catalytic performance for methanol oxidation was also much better than the commercial Pt/C and the Pt/C prepared by impregnation method.

2. Experimental

2.1. Chemicals

The chemical reagent $\text{H}_2\text{PtCl}_6 \cdot 6\text{H}_2\text{O}$ was purchased from Aldrich Chemical Co. The sodium borohydride and ammonium tungstate were purchased from Beijing Chemical Co. The Vulcan Carbon powder XC-72 was purchased from Cabot Corporation (USA). Distilled water ($18.2 \text{ M}\Omega$) was used to prepare the solutions. All the chemicals were of analytical grade and used as received unless otherwise noted.

2.2. Synthesis of Pt/C catalysts

The Pt/C catalyst with 20 wt.% Pt was prepared by the following procedure: An appropriate amount of $(\text{NH}_4)_2\text{WO}_4$ was dissolved in 150 mL of distilled water and then 80 mg of Vulcan XC-72 carbon powder was added into the solution. The mixture was treated in an ultrasonic bath for 30 min, and then $1.43 \text{ mL H}_2\text{PtCl}_6$ solution (72 mmol L^{-1}) was added under vigorous stirring. The obtained mixture was ultrasonicated for another 30 min and continuously stirred for complete reaction between H_2PtCl_6 and $(\text{NH}_4)_2\text{WO}_4$. After that, reduction was performed by dropwise addition of 50 mL freshly prepared aqueous solution of NaBH_4 (30 mmol L^{-1}). Subsequently, the stirring was maintained for 4 h to allow the complete reduction of Pt. Finally, the formed Pt/C catalysts were filtered and washed with hot distilled water until no Cl^- was detected. The supernatant after Pt reduction was colorless, indicating complete reduction of Pt. The Pt/C catalysts were then dried in a vacuum oven at 80°C over night. According to the concentration of $(\text{NH}_4)_2\text{WO}_4$ (0.25 mmol L^{-1} , 0.5 mmol L^{-1} and 1 mmol L^{-1}) used, the catalysts were noted as Pt/C-A, Pt/C-B and Pt/C-C, respectively.

For comparison, a Pt/C catalyst with 20 wt.% Pt noted Pt/C-N catalyst was prepared with the impregnation method. The preparation procedure was similar to the colloidal-precipitation method except that no $(\text{NH}_4)_2\text{WO}_4$ solution was added. A commercial 20 wt.% Pt/C-JM purchased from Aldrich Chemical Co. was noted Pt/C-J as a reference.

2.3. Physical characterization of Pt/C catalysts

The composition of catalysts was estimated by energy dispersive X-ray analysis (EDX) on a JEOL JAX-840 scanning electron microscope operating at 20 kV. X-ray diffraction (XRD) patterns were obtained using a Rigaku-D/MAX-PC 2500 X-ray diffractometer with a $\text{Cu K}\alpha$ ($\lambda = 1.5405 \text{ \AA}$) as radiation source operating at 40 kV and 200 mA. The transmission electron microscope (TEM) images were recorded on a JEOL 2010 TEM system operating at 200 kV. For TEM analysis, the carbon-supported catalyst powders were suspended in ethanol, and a drop of suspension was deposited on a 3 mm-diameter copper grid. X-ray photoelectron spectroscopy (XPS) measurements were carried out using a Kratos XSAM-800 spectrometer with an $\text{Mg K}\alpha$ radiator. The Pt (4f) signals were collected and analyzed with the deconvolution of the spectra using the software XPS peak. All the measurements of the different Pt/C catalysts were carried out three times at the same conditions.

2.4. Electrochemical measurements

The electrocatalytic activity and stability of Pt/C electrodes for methanol oxidation was measured by cyclic voltammetric and chronoamperometric with an EG & G 273 A potentiostat/galvanostat and a conventional three-electrode test cell. A large surface area Pt gauze was served as the counter electrode, and a saturated calomel electrode (SCE) was used as the reference electrode. All potentials in this study were reported with respect to the SCE electrode. The catalysts ink for the electrode preparation was formed by 30 min of ultrasonic mixing of 5 mg catalyst powders with 1 mL of ethanol and 50 μL of Nafion solution (5 wt. %, Aldrich). Subsequently, 10 μL of the catalyst ink was pipetted on a mirror-finished glassy carbon electrode with 3 mm diameter. Finally, the electrode was dried under room temperature for 20 min. The glassy carbon electrode was polished with slurry of 0.5 and 0.03 μm alumina successively and washed ultrasonically in distilled water prior to use. The electrode was first activated in a $0.5 \text{ mol L}^{-1} \text{ H}_2\text{SO}_4$ solution at 50 mV s^{-1} to remove some unstable adsorbed species and increase the reproducibility [30]. The electrochemical CO_{ad} stripping voltammetric experiments were carried out according to literature [31]. The cyclic voltammetric experiments were carried out in a $0.5 \text{ mol L}^{-1} \text{ H}_2\text{SO}_4 + 0.5 \text{ mol L}^{-1} \text{ CH}_3\text{OH}$ solution at 20 mV s^{-1} . The chronoamperometric experiments were performed in a $0.5 \text{ mol L}^{-1} \text{ H}_2\text{SO}_4 + 0.5 \text{ mol L}^{-1} \text{ CH}_3\text{OH}$ solution at 600 mV. The solutions for electrochemical measurements were deaerated by pure nitrogen for 15 min before each experiment. All measurements were carried out at room temperature and the stable results were reported.

3. Results and discussion

3.1. EDX, XRD, TEM and XPS analyses

The EDX spectra for the Pt/C catalysts are shown in Fig. 1A. The mass percentages of Pt for the five catalysts were shown in Table 1, while the Pt loading for Pt/C-A, Pt/C-B and Pt/C-C catalysts were 19.07%, 20.08% and 18.20%, respectively. The Pt loading of the prepared catalysts were consistent with the content of Pt in the precursor, indicating the complete reduction of Pt through the preparation method. The species of tungsten was not found through simply washing with excessive water. However, if the tungsten was present, it won't decrease the catalytic activity because the WO_3 can notably promote the methanol electro-oxidation on Pt catalysts through a hydrogen spillover effect [32–36].

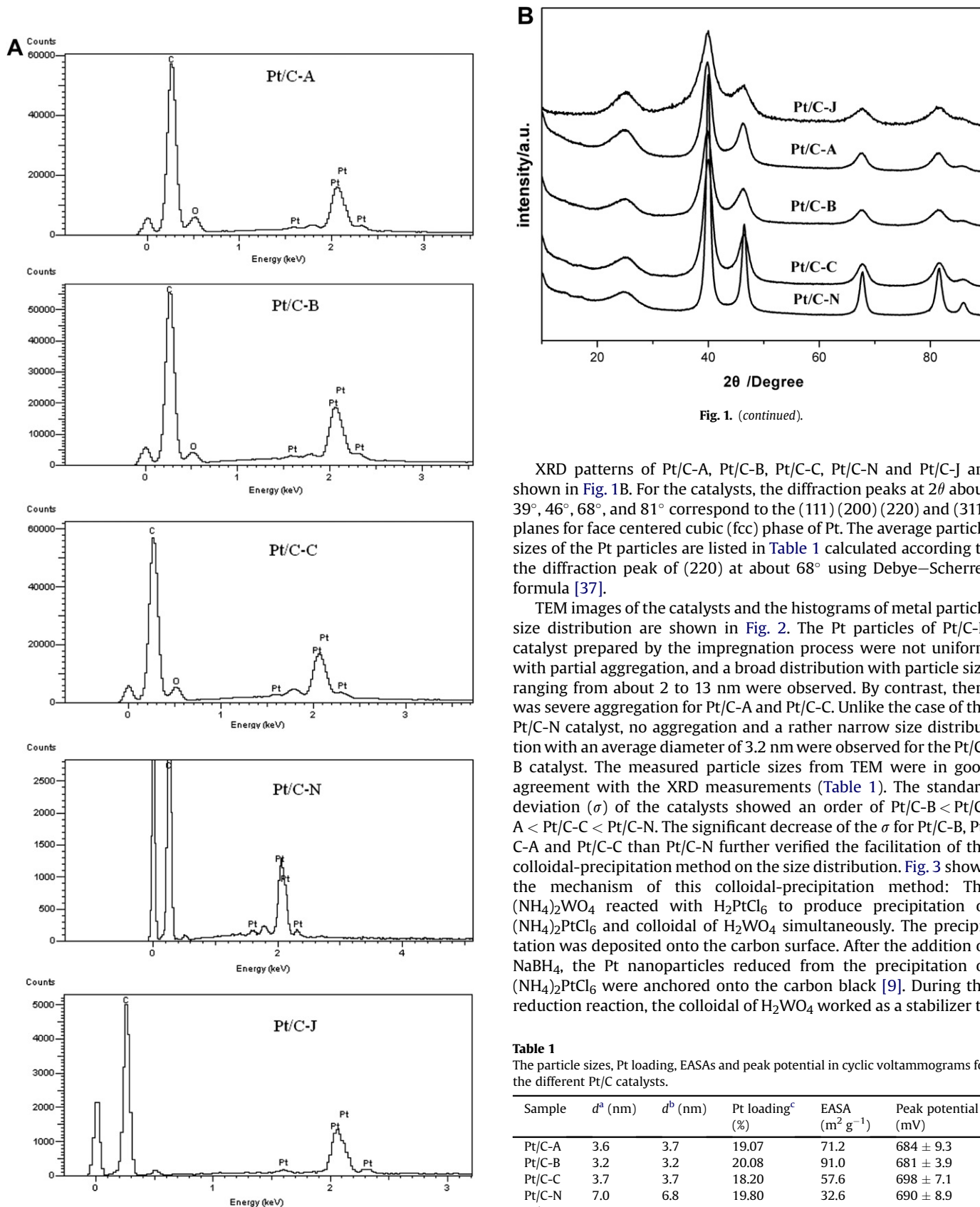


Fig. 1. (continued).

XRD patterns of Pt/C-A, Pt/C-B, Pt/C-C, Pt/C-N and Pt/C-J are shown in Fig. 1B. For the catalysts, the diffraction peaks at 2θ about 39° , 46° , 68° , and 81° correspond to the (111) (200) (220) and (311) planes for face centered cubic (fcc) phase of Pt. The average particle sizes of the Pt particles are listed in Table 1 calculated according to the diffraction peak of (220) at about 68° using Debye–Scherrer formula [37].

TEM images of the catalysts and the histograms of metal particle size distribution are shown in Fig. 2. The Pt particles of Pt/C-N catalyst prepared by the impregnation process were not uniform with partial aggregation, and a broad distribution with particle size ranging from about 2 to 13 nm were observed. By contrast, there was severe aggregation for Pt/C-A and Pt/C-C. Unlike the case of the Pt/C-N catalyst, no aggregation and a rather narrow size distribution with an average diameter of 3.2 nm were observed for the Pt/C-B catalyst. The measured particle sizes from TEM were in good agreement with the XRD measurements (Table 1). The standard deviation (σ) of the catalysts showed an order of Pt/C-B < Pt/C-A < Pt/C-C < Pt/C-N. The significant decrease of the σ for Pt/C-B, Pt/C-A and Pt/C-C than Pt/C-N further verified the facilitation of the colloidal-precipitation method on the size distribution. Fig. 3 shows the mechanism of this colloidal-precipitation method: The $(\text{NH}_4)_2\text{WO}_4$ reacted with H_2PtCl_6 to produce precipitation of $(\text{NH}_4)_2\text{PtCl}_6$ and colloidal of H_2WO_4 simultaneously. The precipitation was deposited onto the carbon surface. After the addition of NaBH_4 , the Pt nanoparticles reduced from the precipitation of $(\text{NH}_4)_2\text{PtCl}_6$ were anchored onto the carbon black [9]. During the reduction reaction, the colloidal of H_2WO_4 worked as a stabilizer to

Table 1

The particle sizes, Pt loading, EASAs and peak potential in cyclic voltammograms for the different Pt/C catalysts.

Sample	d^a (nm)	d^b (nm)	Pt loading ^c (%)	EASA ($\text{m}^2 \text{g}^{-1}$)	Peak potential (mV)
Pt/C-A	3.6	3.7	19.07	71.2	684 ± 9.3
Pt/C-B	3.2	3.2	20.08	91.0	681 ± 3.9
Pt/C-C	3.7	3.7	18.20	57.6	698 ± 7.1
Pt/C-N	7.0	6.8	19.80	32.6	690 ± 8.9
Pt/C-J	3.0	2.9	20.56	118	702 ± 5.4

^a The particle sizes of Pt calculated from XRD patterns according to Debye–Scherrer formula.

^b The average particle sizes obtained from TEM images.

^c The Pt loading obtained from EDX spectra.

Fig. 1. EDX spectra (A) and XRD pattern (B) of different catalysts.

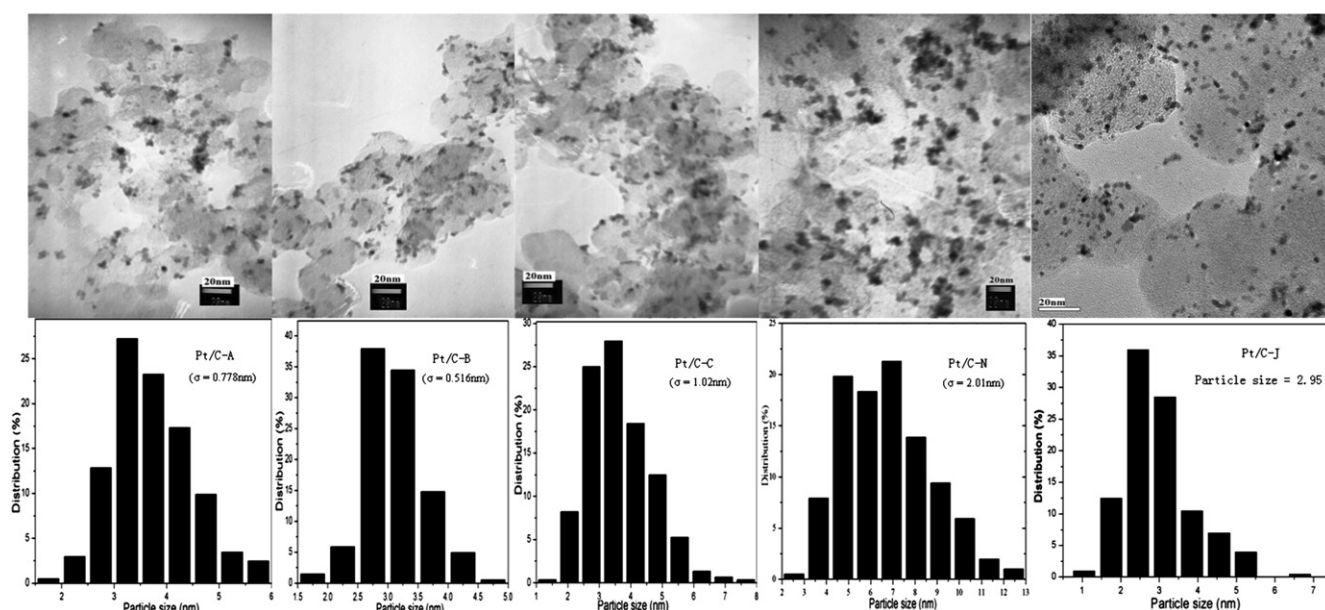


Fig. 2. TEM images and size distribution histograms of the Pt/C-A, Pt/C-B, Pt/C-C, Pt/C-N and Pt/C-J catalysts: The bars in the images indicate a 20 nm scale.

prevent the particles from aggregation. Nanoparticles with a narrow distribution and uniform size can thus be prepared. Takasu et al. [38] have studied the size effect of catalysts for DMFC. According to their study, a particle size of ~ 3 nm could yield maximum mass-specific activity toward methanol electro-oxidation. The average sizes for the as-prepared Pt nanoparticles of Pt/C-A, Pt/C-B and Pt/C-C is 3.7, 3.2 and 3.7, respectively, which are all near 3 nm. So the as-prepared catalysts are expected to show good performance for methanol electrooxidation. Considering these results, fine and stable noble-metal nanoparticles can be prepared by this colloidal-precipitation method, and the best one with good particles dispersion was obtained by the stabilization of $0.5 \text{ mmol L}^{-1} (\text{NH}_4)_2\text{WO}_4$.

Fig. 4 shows the XPS spectra of the Pt/C-B, Pt/C-N and Pt/C-J catalysts. For Pt/C-B, the Pt $4f_{7/2}$ peak at 71.8 eV and Pt $4f_{5/2}$ peak at 75.1 eV belong to Pt^0 , while the Pt $4f_{7/2}$ peak at 73.2 eV and Pt $4f_{5/2}$ peak at 76.4 eV are assigned to Pt^{2+} in PtO or $\text{Pt}(\text{OH})_2$ [39]. The binding energy is in good agreement with data from the NIST XPS database [40]. While the peaks for Pt/C-N and Pt/C-J are nearly the same as that of Pt/C-B except a slight negative shift was observed for Pt/C-N as shown in the figure. The percentages of the Pt^0 species were calculated from the relative areas of the $4f_{7/2}$ peaks and the percentages were 58%, 56% and 57% for Pt/C-B, Pt/C-N and Pt/C-J, respectively.

3.2. Electrochemical analysis

The electrochemical active surface area (EASA) of a catalyst can reflect the intrinsic electrocatalytic activity of the catalyst. Usually, it

can be measured with the H_{ad} stripping or CO_{ad} stripping method [10]. Here, Fig. 5 shows the CO_{ad} stripping voltammograms for the Pt/C catalysts. The surface area of Pt metal was estimated assuming that the coulombic charge necessary for oxidation of a monolayer of linearly adsorbed CO was $420 \mu\text{C cm}^{-2}$ [10,41]. Clearly, both the onset potential and peak potential of the home-made Pt/C catalysts prepared by colloidal-precipitation method shifted negatively compare with the Pt/C-J, indicating that the CO adsorptive bond on the Pt sites was weakened. CO_{ad} is considered to be the poison special according to the dual pathway mechanism [42,43], in which CO_{ad} can occupy the Pt sites and lead to a decrease in reaction kinetics. Weakened CO_{ad} adsorption facilitates the release of the Pt active sites, promising better CO tolerance and higher performance. The EASAs of the catalysts calculated from the area of the CO_{ad} oxidation peak are shown in Table 1. The EASAs of the catalysts showed an order of $\text{Pt/C-N} < \text{Pt/C-C} < \text{Pt/C-A} < \text{Pt/C-B} < \text{Pt/C-J}$. According to the data, the EASAs of the as-prepared catalysts was a little smaller than Pt/C-J. However, it is more reasonable to compare the as-prepared catalysts with the Pt/C-N catalyst. The EASAs of the three catalysts were all much larger than that of Pt/C-N.

Fig. 6A displays the cyclic voltammograms (CVs) for the Pt/C catalysts by colloidal-precipitation method. Clearly, the Pt/C-B catalyst showed the highest peak current, indicating a best activity for methanol electrooxidation. The result agreed well with the data of TEM and CO_{ad} stripping voltammetric experiment listed in Table 1, in which the Pt/C-B catalyst showed the smallest particle size and the highest EASA. It can be concluded that the Pt/C-B catalyst was the best one for methanol electrooxidation among the three as-prepared catalysts. The CVs for Pt/C-B, Pt/C-J and Pt/C-

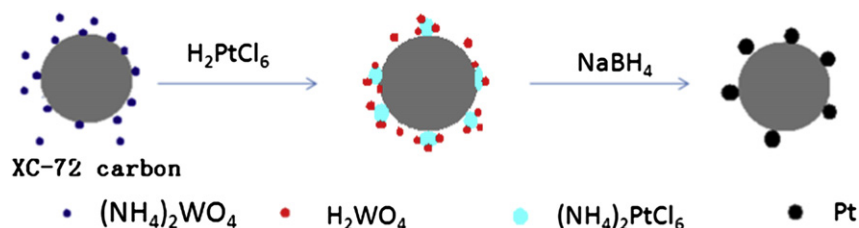


Fig. 3. An illustration for the preparation of Pt/C catalysts by the colloidal-precipitation method.

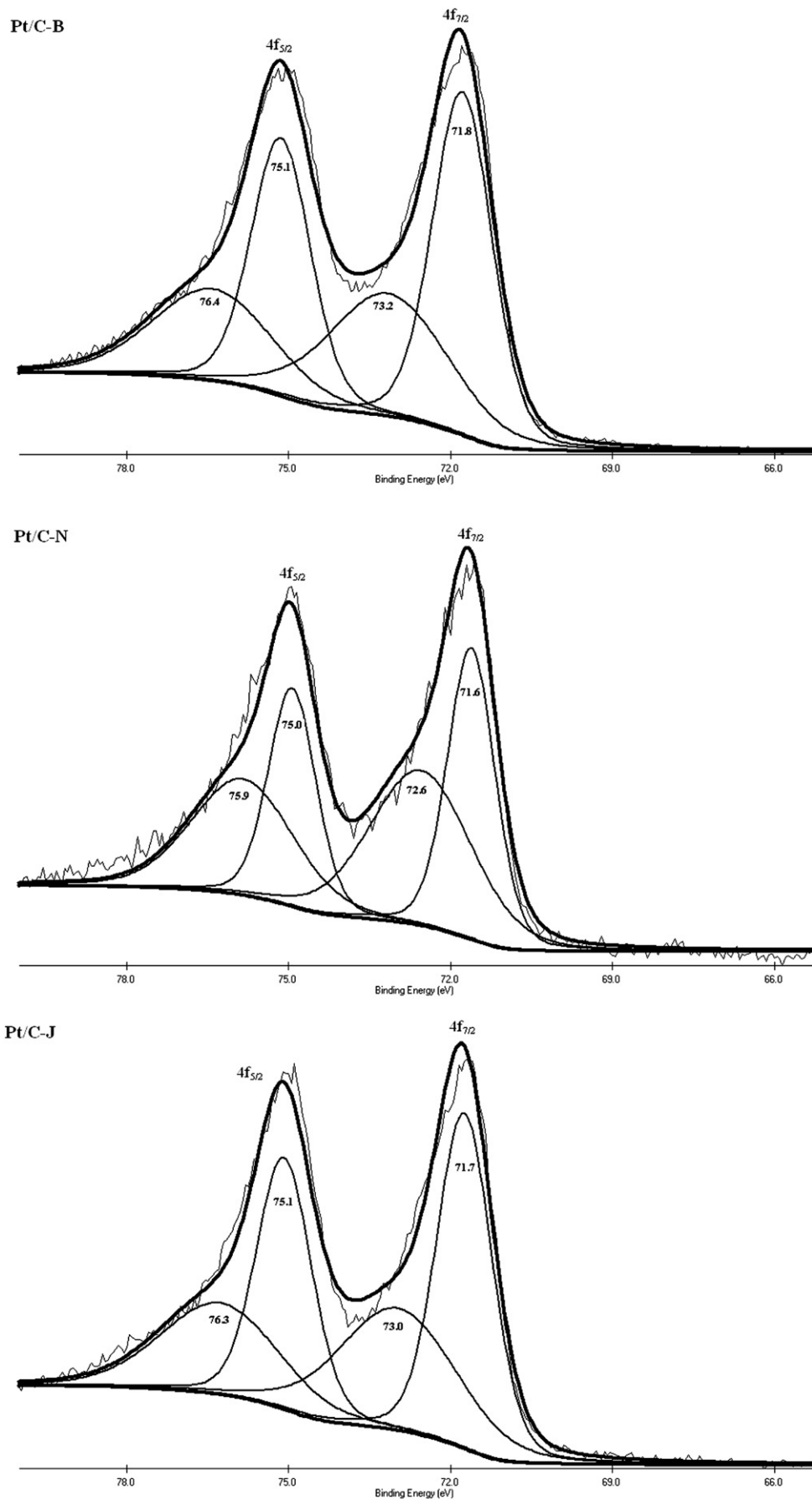


Fig. 4. XPS data of Pt (4f) for the Pt/C-B, Pt/C-N and Pt/C-J catalysts.

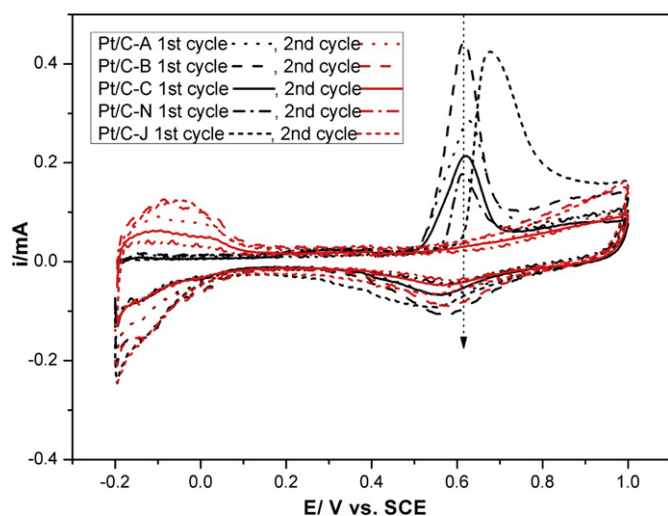


Fig. 5. CO_{ad} stripping voltammograms of Pt/C-A, Pt/C-B, Pt/C-C, Pt/C-N and Pt/C-J catalysts in a $0.5 \text{ mol L}^{-1} \text{H}_2\text{SO}_4$ solution at a scan rate of 20 mV s^{-1} .

N are shown in Fig. 6B. It can be observed that the corresponding onset potential and peak potential of the Pt/C-B shifted negatively compared to the commercial Pt/C catalyst, especially in the range of $0.2\text{--}0.6 \text{ V}$. The peak current of the three catalysts were $413 \text{ mA mg}^{-1}\text{Pt}$, $332 \text{ mA mg}^{-1}\text{Pt}$ and $110 \text{ mA mg}^{-1}\text{Pt}$ for Pt/C-B,

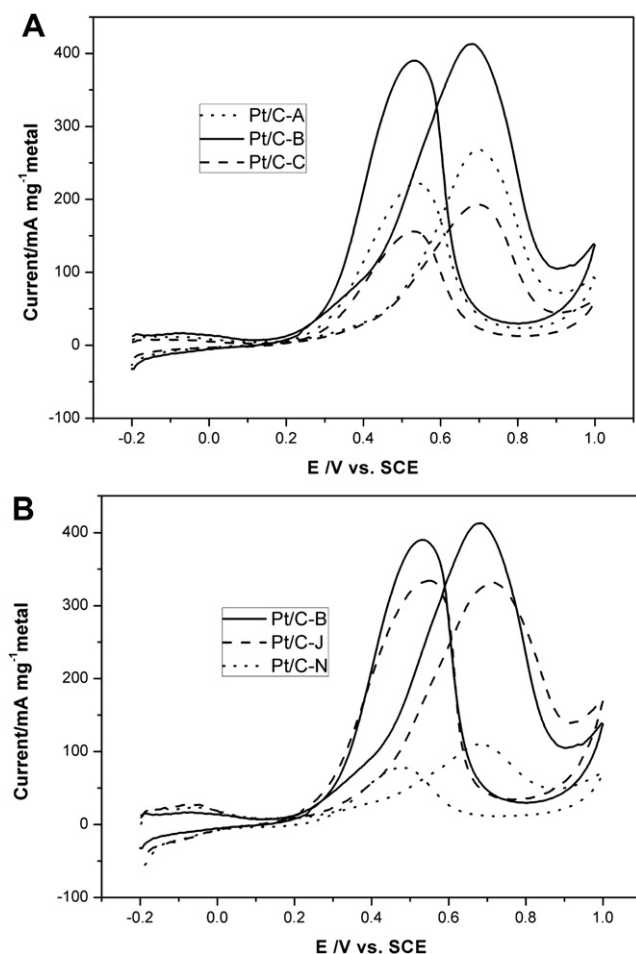


Fig. 6. Cyclic voltammograms for Pt/C-A, Pt/C-B and Pt/C-C catalysts in $0.5 \text{ mol L}^{-1} \text{H}_2\text{SO}_4 + 0.5 \text{ mol L}^{-1} \text{CH}_3\text{OH}$ solution at 20 mV s^{-1} (A), and cyclic voltammograms for Pt/C-B, Pt/C-N and Pt/C-J catalysts (B).

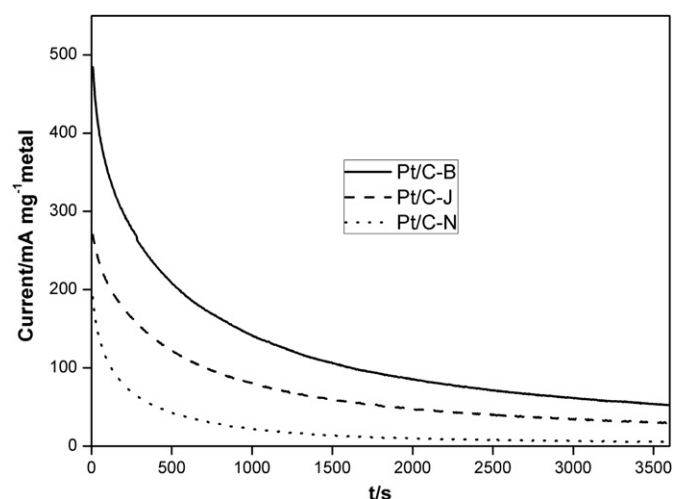


Fig. 7. Chronoamperometric curves for Pt/C-B, Pt/C-N and Pt/C-J catalysts in $0.5 \text{ mol L}^{-1} \text{H}_2\text{SO}_4 + 0.5 \text{ mol L}^{-1} \text{CH}_3\text{OH}$ solution at 0.6 V .

Pt/C-J and Pt/C-N, respectively. While the peak current for the JM Pt catalyst was reported to be $152\text{--}618 \text{ mA mg}^{-1}\text{Pt}$ [44–46] depending on the test conditions. The MSA was calculated by integration of the charge density corresponding for methanol oxidation divided by metal loading to evaluate the electrocatalytic activities according to the following equation [47,48]:

$$\text{MSA} = \frac{Q_{\text{MOR}}}{L_{\text{Pt}}}$$

where the MSA is the mass specific activity for MOR (mC mg^{-1}), Q_{MOR} is the charge density for methanol oxidation peak (mC cm^{-2}) and L_{Pt} is the loading of Pt in the electrode (mg cm^{-2}). The calculated MSA for Pt/C-B (4750 mC mg^{-1}) was 48% higher than that of Pt/C-J (3200 mC mg^{-1}). Moreover, the performance of the catalysts was affected by some factors such as the structure, composition, and morphology and preparation method, so it is more reasonable to compare the Pt catalysts produced by the same method. And the MSA for Pt/C-B was almost 4 fold enhanced than the MSA for Pt/C-N (880 mC mg^{-1}).

Chronoamperometric (CA) curves for the Pt/C-B, Pt/C-J and Pt/C-N catalysts are shown in Fig. 7. These curves reflect the activity and stability of the three catalysts for methanol oxidation. Evidently, the Pt/C-B catalyst showed the highest initial current density and best stability. Due to the double layer charging, or intermediates accumulation in the above electrochemical tests [49], it was more reasonable to compare the catalytic stability by the limiting current or the steady-state current after 500 s. At 3600 s, the current for catalysts exhibited in a notable order of $\text{Pt/C-B} > \text{Pt/C-J} > \text{Pt/C-N}$, the value for the Pt/C-B catalyst was $52.6 \text{ mA mg}^{-1}\text{Pt}$, approximately 1.78 times of that at the state-of-the-art Pt/C-J. This result coincided with the CO_{ad} stripping voltammograms in which the poisoning species of CO_{ad} was easily oxidized at the catalysts prepared by colloidal-precipitation method. Considering the results, the simple colloidal-precipitation method greatly increased the catalytic activity and stability for methanol electrooxidation.

4. Conclusion

A novel and simple colloidal-precipitation method has been explored to prepare Pt/C catalysts with a narrow size distribution for methanol electrooxidation successfully. The size of the Pt nanoparticles can be effectively controlled by changing the

concentration of $(\text{NH}_4)_2\text{WO}_4$. Physical characterization showed that the best concentration of $(\text{NH}_4)_2\text{WO}_4$ was 0.5 mmol L^{-1} and the prepared Pt nanoparticles were well dispersed on the carbon support with an average size of 3.2 nm and a narrow size distribution of $\sigma = 0.516$. Electrochemical measurements showed that the as-prepared Pt/C catalyst had higher catalytic activity and better stability for methanol electrooxidation than both the normal Pt/C and the commercial Pt/C catalysts.

Acknowledgements

This work was supported by the General Programs of National Natural Science Foundation of China (20876153, 21073180), the Science & Technology Research Programs of Jilin Province (20100420), the High Technology Research Program (863 program, 2007AA05Z159) of the Science and Technology Ministry of China, International (Regional) Cooperation and Exchange program of National Natural Science Foundation of China (2101130027), National Basic Research Program of China (973 Program, Nos. 2012CB932802 and 2012CB215500).

References

- [1] Z.R. Shen, M. Yamada, M. Miyake, *Chemical Communications* (2007) 245–247.
- [2] L. Feng, J. Zhang, W. Cai, Liangliang, W. Xing, C. Liu, *Journal of Power Sources* 196 (2011) 2750–2753.
- [3] L. Feng, X. Zhao, J. Yang, W. Xing, C. Liu, *Catalysis Communications* 14 (2011) 10–14.
- [4] L. Feng, Q. Lv, X. Sun, S. Yao, C. Liu, W. Xing, *Journal of Electroanalytical Chemistry* 664 (2012) 14–19.
- [5] S. Surampudi, S.R. Narayanan, E. Vamos, H. Frank, G. Halpert, A. Laconti, J. Kosek, G.K.S. Prakash, G.A. Olah, *Journal of Power Sources* 47 (1994) 377–385.
- [6] T.J. Schmidt, M. Noeske, H.A. Gasteiger, R.J. Behm, P. Britz, W. Brijoux, H. Bonnemann, *Langmuir* 13 (1997) 2591–2595.
- [7] A.S. Arico, V. Baglio, A. Di Blasi, E. Modica, P.L. Antonucci, V. Antonucci, *Journal of Electroanalytical Chemistry* 557 (2003) 167–176.
- [8] X.Z. Xue, J.J. Ge, T. Tian, C.P. Liu, W. Xing, T.H. Lu, *Journal of Power Sources* 172 (2007) 560–569.
- [9] C.P. Liu, X.Z. Xue, T.H. Lu, W. Xing, *Journal of Power Sources* 161 (2006) 68–73.
- [10] Y. Takasu, T. Fujiwara, Y. Murakami, K. Sasaki, M. Oguri, T. Asaki, W. Sugimoto, *Journal of the Electrochemical Society* 147 (2000) 4421–4427.
- [11] A. Lekhal, B.J. Glasser, J.G. Khinast, *Chemical Engineering Science* 59 (2004) 1063–1077.
- [12] Z.M. Cui, C.P. Liu, J.H. Liao, W. Xing, *Electrochimica Acta* 53 (2008) 7807–7811.
- [13] M.K. Jeon, P.J. McGinn, *Journal of Power Sources* 195 (2010) 2664–2668.
- [14] K. Balakrishnan, R.D. Gonzalez, *Langmuir* 10 (1994) 2487–2490.
- [15] J.Y. Kim, Z.G. Yang, C.C. Chang, T.I. Valdez, S.R. Narayanan, P.N. Kumta, *Journal of the Electrochemical Society* 150 (2003) A1421–A1431.
- [16] H. Bonnemann, W. Brijoux, R. Brinkmann, E. Dinjus, T. Jousen, B. Korall, *Angewandte Chemie-International Edition in English* 30 (1991) 1312–1314.
- [17] U.A. Paulus, U. Endruschat, G.J. Feldmeyer, T.J. Schmidt, H. Bonnemann, R.J. Behm, *Journal of Catalysis* 195 (2000) 383–393.
- [18] Y.J. Huang, X.C. Zhou, J.H. Liao, C.P. Liu, T.H. Lu, W. Xing, *Electrochemistry Communications* 10 (2008) 621–624.
- [19] I. Lee, R. Morales, M.A. Albiter, F. Zaera, *Proceedings of the National Academy of Sciences of the United States of America* 105 (2008) 15241–15246.
- [20] N.C. Bigall, A. Eychmuller, *Philosophical Transactions of the Royal Society A-Mathematical Physical and Engineering Sciences* 368 (2010) 1385–1404.
- [21] H.H. Ingelsten, J.C. Beziat, K. Bergkvist, A. Palmqvist, M. Skoglundh, Q.H. Hu, L.K.L. Falk, K. Holmberg, *Langmuir* 18 (2002) 1811–1818.
- [22] X. Zhang, K.Y. Chan, *Chemistry of Materials* 15 (2003) 451–459.
- [23] M. Chen, Y.G. Feng, L.Y. Wang, L. Zhang, J.Y. Zhang, *Colloids and Surfaces A Physicochemical and Engineering Aspects* 281 (2006) 119–124.
- [24] X. Li, W.X. Chen, J. Zhao, W. Xing, Z.D. Xu, *Carbon* 43 (2005) 2168–2174.
- [25] M.S. Wilson, S. Gottesfeld, *Journal of the Electrochemical Society* 139 (1992) L28–L30.
- [26] Z.L. Liu, X.Y. Ling, J.Y. Lee, X.D. Su, L.M. Gan, *Journal of Materials Chemistry* 13 (2003) 3049–3052.
- [27] T. Kim, M. Takahashi, M. Nagai, K. Kobayashi, *Electrochimica Acta* 50 (2004) 817–821.
- [28] F. Bensebaa, N. Patrito, Y. Le Page, P. L'Ecuyer, D.S. Wang, *Journal of Materials Chemistry* 14 (2004) 3378–3384.
- [29] H. Bonnemann, K.S. Nagabhushana, *Journal of New Materials for Electrochemical Systems* 7 (2004) 93–108.
- [30] A.B. Kashyout, A.B.A. Nassr, L. Giorgi, T. Maiyalagan, B.A.B. Youssef, *International Journal of Electrochemical Science* 6 (2011) 379–393.
- [31] X.Z. Xue, T.H. Lu, C.P. Liu, W.L. Xu, Y. Su, Y.Z. Lv, W. Xing, *Electrochimica Acta* 50 (2005) 3470–3478.
- [32] P.J. Kulesza, L.R. Faulkner, *Journal of Electroanalytical Chemistry* 259 (1989) 81–98.
- [33] P. Shen, K. Chen, A.C.C. Tseung, *Journal of the Chemical Society, Faraday Transactions* 90 (1994) 3089–3096.
- [34] K.W. Park, J.H. Choi, K.S. Ahn, Y.E. Sung, *Journal of Physical Chemistry B* 108 (2004) 5989–5994.
- [35] S. Jayaraman, T.F. Jaramillo, E.W. McFarland, *Abstracts of Papers American Chemical Society* 229 (2005). 845-INOR.
- [36] Z.M. Cui, L.G. Feng, C.P. Liu, W. Xing, *Journal of Power Sources* 196 (2011) 2621–2626.
- [37] X.M. Wang, Y.Y. Xia, *Electrochemistry Communications* 11 (2009) 28–30.
- [38] Y. Takasu, H. Itaya, T. Iwazaki, R. Miyoshi, T. Ohnuma, W. Sugimoto, Y. Murakami, *Chemical Communications* (2001) 341–342.
- [39] Y. Baer, et al., *Physica Scripta* 1 (1970) 55.
- [40] U. S. National Institute of Standards and Technology (NIST) XPS database, can be found under <http://srdata.nist.gov/xps/> and references therein.
- [41] T. Kawaguchi, *Electrochemistry Communications* 6 (2004) 480.
- [42] M.W. Breiter, *Journal of Electroanalytical Chemistry* 15 (1967) 221.
- [43] M.W. Breiter, *Journal of Electroanalytical Chemistry* 14 (1967) 407.
- [44] J.W. Chen, C.P. Jiang, X. Yang, L. Feng, E.B. Gallogly, R.L. Wang, *Electrochemistry Communications* 13 (2011) 314–316.
- [45] R. Lv, T. Cui, M.-S. Jun, Q. Zhang, A. Cao, D.S. Su, Z. Zhang, S.-H. Yoon, J. Miyawaki, I. Mochida, F. Kang, *Advanced Functional Materials* 21 (2011) 999–1006.
- [46] C. Hu, Y. Guo, Y. Cao, L. Yang, Z. Bai, K. Wang, P. Xu, J. Zhou, *Materials Science and Engineering B-Advanced Functional Solid-State Materials* 176 (2011) 1467–1473.
- [47] L. Giorgi, T.D. Makris, R. Giorgi, N. Lisi, E. Salernitano, *Sensors and Actuators B Chemical* 126 (2007) 144–152.
- [48] C. Paoletti, A. Cemmi, L. Giorgi, R. Giorgi, L. Pilloni, E. Serra, M. Pasquali, *Journal of Power Sources* 183 (2008) 84–91.
- [49] Z.-B. Wang, G.-P. Yin, P.-F. Shi, B.-Q. Yang, P.-X. Feng, *Journal of Power Sources* 166 (2007) 317–323.